



A Journal of



Accepted Article

Title: Dehydrogenation of Formic Acid Catalyzed by Water-Soluble Ruthenium Complexes: X-ray Crystal Structure of a Diruthenium Complex

Authors: Soumyadip Patra, Mahendra K. Awasthi, Rohit K. Rai, Hemanta Deka, Shaikh M. Mobin, and Sanjay Kumar Singh

This manuscript has been accepted after peer review and appears as an Accepted Article online prior to editing, proofing, and formal publication of the final Version of Record (VoR). This work is currently citable by using the Digital Object Identifier (DOI) given below. The VoR will be published online in Early View as soon as possible and may be different to this Accepted Article as a result of editing. Readers should obtain the VoR from the journal website shown below when it is published to ensure accuracy of information. The authors are responsible for the content of this Accepted Article.

To be cited as: *Eur. J. Inorg. Chem.* 10.1002/ejic.201801501

Link to VoR: <http://dx.doi.org/10.1002/ejic.201801501>

WILEY-VCH

Dehydrogenation of Formic Acid Catalyzed by Water-Soluble Ruthenium Complexes: X-ray Crystal Structure of a Diruthenium Complex

Soumyadip Patra,^[a] Mahendra K. Awasthi,^[a] Dr. Rohit K. Rai,^[a] Dr. Hemanta Deka,^[a] Dr. Shaikh M. Mobin^[a] and Dr. Sanjay K. Singh*^[a]

^[a] Discipline of Chemistry, Indian Institute of Technology Indore, Simrol, Indore 453552, India

E-mail: sksingh@iiti.ac.in

URL: <http://people.iiti.ac.in/~sksingh/>

ABSTRACT

Dehydrogenation of formic acid over various Ru-arene complexes containing N-donor chelating ligands was investigated in H₂O and isolated and characterized several important catalytic intermediate species to elucidate the reaction pathway for formic acid dehydrogenation. Among the studied complexes, Ru-arene complexes, namely $[(\eta^6\text{-C}_6\text{H}_6)\text{Ru}(\kappa^2\text{-N}_{\text{py}}\text{NH}_2\text{-AmQ})\text{Cl}]^+$ (**C-2**), $[(\eta^6\text{-C}_{10}\text{H}_{14})\text{Ru}(\kappa^2\text{-N}_{\text{py}}\text{NH}_2\text{-AmQ})\text{Cl}]^+$ (**C-3**) and $[(\eta^6\text{-C}_6\text{H}_6)\text{Ru}(\kappa^2\text{-N}_{\text{py}}\text{NHMe-MAmQ})\text{Cl}]^+$ (**C-4**) (AmQ = 8-aminoquinoline and MAmQ = 8-(N-methylamino)quinoline) were proved to be the efficient catalysts for formic acid dehydrogenation at 90 °C, even in the absence of base. With an initial TOF of 940 h⁻¹, complex **C-4** displayed the highest catalytic activity for formic acid dehydrogenation in H₂O and it can be recycled up to 5 times with a TON of 2248. Effect of temperature, pH, formic acid and catalyst concentration on the reaction kinetics were also investigated in detail. Extensive mechanistic investigations using mass spectrometry and NMR evidenced the formation of a coordinatively unsaturated species $[(\eta^6\text{-C}_6\text{H}_6)\text{Ru}(\kappa^2\text{-N}_{\text{py}}\text{NH-AmQ})]^+$ (**C-2A**) / $[(\eta^6\text{-C}_6\text{H}_6)\text{Ru}(\kappa^2\text{-N}_{\text{py}}\text{NMe-MAmQ})]^+$ (**C-4A**) as the active component during the catalytic dehydrogenation of formic acid. We further characterized the dimer-form of **C-2A**, possibly the catalyst resting state, by single crystal X-ray crystallography.

Keywords: dehydrogenation, formic acid, sodium formate, reaction mechanism, 8-aminoquinoline.

INTRODUCTION

In the modern era, there prevails a huge demand to supply gap concerning the energy resources and hence the quest for green and renewable energy sources to meet the global energy demand is one of the key challenges of the society. In this context, hydrogen (H₂) is emerging as a clean alternative source of energy, as only H₂O is produced by its reaction in fuel cells.^[1,2] However, the extremely explosive nature of H₂ and the difficulty in its transportation lead to the search for suitable hydrogen storage compounds, which are safer to handle, can be transported easily and release H₂ under mild conditions.^[3] In this regard, formic acid being a liquid under ambient conditions has attracted considerable interest, as it can be handled, stored and transported easily and safely.^[4] In the presence of a suitable catalyst, formic acid generates H₂ and CO₂, under relatively mild reaction condition.

After one of the first reports on formic acid dehydrogenation over Ir-phosphine complex in 1967 by Coffey,^[5] this reaction has been investigated extensively only in the recent past. Several transition metal complexes based on iron,^[6] rhodium,^[7] ruthenium^[8,9] and iridium^[10-14] have been particularly proven to be active catalysts for formic acid dehydrogenation. Notably, ancillary ligands play an important role in tuning the catalytic activity of these metal catalysts for formic acid dehydrogenation. For instance, a strong σ -donor ligand enhances the electron density at the metal center, and such electron-rich metals are found to be the favorable site for efficient activation of formic acid to CO₂ and H₂.^[4j,10s] Moreover, the protic ligands are of particular importance in formic acid dehydrogenation reactions, as these ligands enhance the dehydrogenation pathway by involving in hydrogen bond interactions with the solvent or formic acid.^[4k,10c,10d,10g,10m-o] For example, iridium complexes bearing proton responsive ligands have been found to be particularly active for formic acid dehydrogenation in H₂O.^[11-13] Himeda *et al.* reported the catalyst [Cp*Ir(4,4'-

DHBP)(H₂O)]SO₄ with the TOF of 14000 h⁻¹.^[13] The same group afterwards reported the catalyst [Cp*Ir(TMBI)H₂O]SO₄ with a TOF of 34000 h⁻¹.^[10e] In 2015, Himeda *et al.* further improved the results by developing the catalyst [Cp*Ir(pyrimidylimidazoline)H₂O]SO₄ which gave a TOF of 322000 h⁻¹ in HCOOH/HCOONa aqueous solution.^[10q] Li *et al.* developed the catalyst [Ir(η⁵-C₅Me₅)Cl(2,2'-bi-2-imidazole)]⁺ with the TOF of 487500 h⁻¹.^[11] Very recently, this group has reported a new iridium-based catalyst bearing a dioxime derived ligand which gave a record TON of 5020000 at 70 °C.^[10l] Joo *et al.* reported an iridium hydride complex which gave a TOF of 298000 h⁻¹ at 100 °C in formic acid dehydrogenation.^[10u] Some of the other premier results obtained for formic acid dehydrogenation especially in aqueous medium have been listed in the supporting information (Table S1). Although iridium-based catalysts have been proven to be very active in formic acid dehydrogenation, its price prompts us to look for a more economical option. Literature reports revealed that ruthenium-based catalysts except a few such as [Ru(η⁶-C₁₀H₁₄)Cl(2,2'-bi-2-imidazole)]⁺ and [Ru(H₂O)₆](tos)₂/TPPTS (tos = *p*-toluene sulfonate and TPPTS = *m*-trisulfonated triphenylphosphine) have all been tested in organic solvents for formic acid dehydrogenation.^[8a,8g-8j,9,15,16] Higher activities of the complexes [Ir(η⁵-C₅Me₅)Cl(2,2'-bi-2-imidazole)]⁺ and [Ru(η⁶-C₁₀H₁₄)Cl(2,2'-bi-2-imidazole)]⁺ for formic acid dehydrogenation suggest the importance of N-H moieties on the catalytic activity.^[9,11]

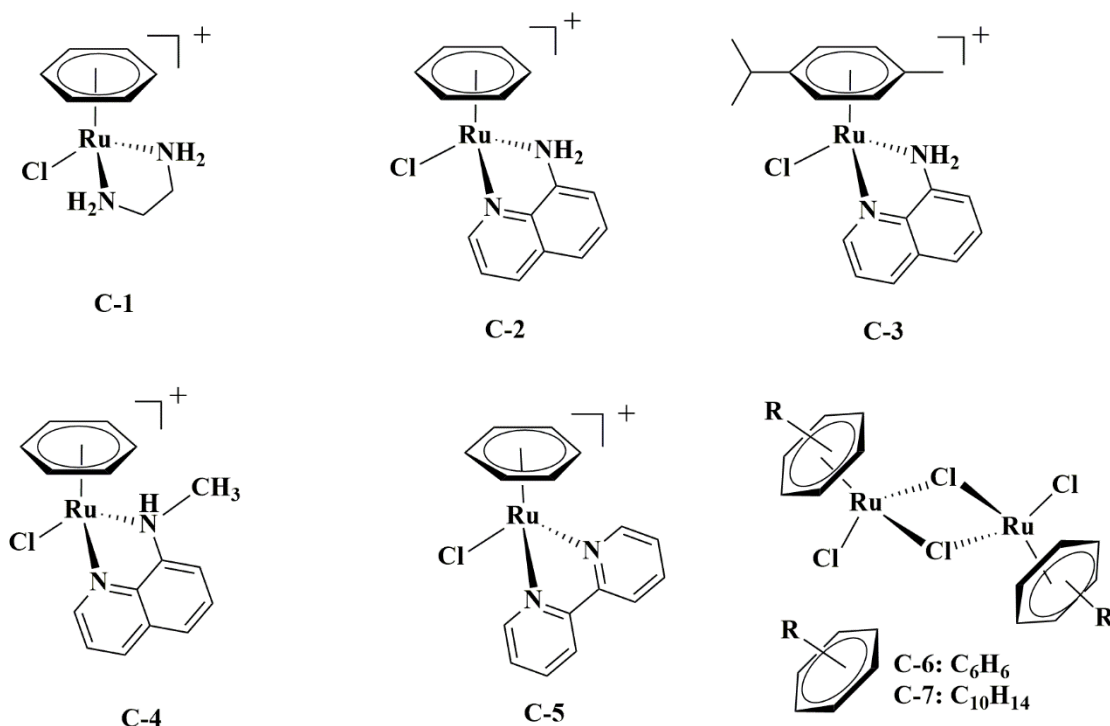
In one of our recent findings, we observed that Ru-arene complexes containing ethylenediamine (en) and 8-aminoquinoline (AmQ) based chelating ligands efficiently catalyzed the furfural to levulinic acid (LA) transformation with the aid of formic acid. We demonstrated that the N-H moieties of en and AmQ ligands play a crucial role in the initial activation of formic acid to facilitate the transfer hydrogenation of furfural to furfuryl alcohol, which eventually transformed to LA.^[17,18] Very recently, Oro *et al.* reported Ir-NHC

(NHC = N-heterocyclic carbene) based complexes for formic acid dehydrogenation in DMF and H₂O.^[14] Though these complexes exhibit only moderate activity in H₂O, the initial TOF is highest (790 h⁻¹) for the Ir-NHC-AmQ complex. Moreover, a significant quenching of the catalytic activity of Ir-NHC complex was observed when AmQ was replaced with 8-(N, N-dimethylamino)quinoline (DMAmQ), suggesting the crucial role of NH moiety of AmQ in enhancing the catalytic activity for formic acid dehydrogenation in H₂O. Envisioned by our previous observations, herein, we investigated in detail the dehydrogenation of formic acid over Ru-arene complexes containing various nitrogen-donor chelating ligands and demonstrated the crucial role of these ligands on the formic acid dehydrogenation process. Moreover, mechanistic insights were elaborated by identifying several catalytic intermediates involved in various steps of the catalytic dehydrogenation of formic acid under the catalytic and controlled reaction conditions. Most importantly, the structure of a diruthenium species, possibly the catalyst resting state, was established by X-ray crystallography.

RESULTS AND DISCUSSION

Complexes $[(\eta^6\text{-C}_6\text{H}_6)\text{Ru}(\kappa^2\text{-NH}_2\text{NH}_2\text{-en})\text{Cl}]^+$ (**C-1**), $[(\eta^6\text{-C}_6\text{H}_6)\text{Ru}(\kappa^2\text{-N}_{\text{py}}\text{NH}_2\text{-8-AmQ})\text{Cl}]^+$ (**C-2**) and $[(\eta^6\text{-C}_{10}\text{H}_{14})\text{Ru}(\kappa^2\text{-N}_{\text{py}}\text{NH}_2\text{-8-AmQ})\text{Cl}]^+$ (**C-3**) shown in Scheme 1 were synthesized from the precursor $[(\eta^6\text{-arene})\text{RuCl}_2]_2$ (**C-6** and **C-7**) and the suitable ligands following our previously reported method.^[17,18] Complex $[(\eta^6\text{-C}_6\text{H}_6)\text{Ru}(\kappa^2\text{-N}_{\text{py}}\text{NHMe-8-AmQ})\text{Cl}]^+$ (**C-4**) was obtained at room temperature from the reaction of the precursor $[(\eta^6\text{-benzene})\text{RuCl}_2]_2$ (**C-6**) and the ligand 8-(N-methylamino)quinoline (MAmQ) (Scheme 1 and Schemes S1-S2). Complex $[(\eta^6\text{-C}_6\text{H}_6)\text{Ru}(\kappa^2\text{-bpy})\text{Cl}]^+$ (**C-5**) was also synthesized from the reaction of $[(\eta^6\text{-benzene})\text{RuCl}_2]_2$ (**C-6**) and 2,2'-bipyridine (bpy), to evaluate the role of NH in formic acid dehydrogenation.

For the initial screening of active catalysts, formic acid dehydrogenation over complexes **C-1** – **C-5** (1 mol %) and the precursor **C-6** – **C-7** (0.5 mol %) was investigated using 0.4 M formic acid (aq.) solution (2.5 mL) and sodium formate (5 mol%) at 90 °C (Table 1, entries 1-7). The amount of the evolved gases was measured by water displacement method, and the release of H₂ and CO₂ gas was confirmed by GC-TCD (Figure S1). Preliminary results inferred that the complexes **C-2** – **C-4** containing 8-aminoquinoline based ligands were much more efficient than the complex **C-1** containing ethylenediamine ligand for formic acid dehydrogenation reaction (Table 1, entries 1-4 and Figure S2). The only marginal increment in the TOF of complex **C-2** over **C-3** suggests that the arene-ring offer no significant enhancement in formic acid dehydrogenation. Among the related complexes, the TOF for formic acid dehydrogenation over **C-4** (TOF 364 h⁻¹) was found to be 4-fold higher than the complex **C-2** (TOF 83 h⁻¹) (Table 1, entries 2 and 4). On the other hand, the [(η⁶-C₆H₆)Ru(κ²-bpy)Cl]⁺ (**C-5**) display only poor activity (Table 1, entry 5). Notably, the precursor complexes **C-6** and **C-7**, lacking any nitrogen-based ligands, are also poorly active (Table 1, entries 6 and 7). These findings suggest the importance of protic ligands, availability of NH moiety and the stability of the catalyst for the catalytic formic acid dehydrogenation reaction.



Scheme 1. Complexes C-1 – C-7 explored for the dehydrogenation of formic acid

Table 1. Catalytic dehydrogenation of formic acid over various catalysts ^[a] .				
$\text{HCOOH} \xrightarrow[\text{HCOONa, H}_2\text{O, 90 }^\circ\text{C}]{\text{Ru-catalyst}} \text{H}_2 + \text{CO}_2$				
Entry	Catalyst	Conv. (%) ^[b]	TON ^[d]	TOF (h ⁻¹) ^[d]
1	C-1	90	90	53
2	C-2	91	91	83
3	C-3	90	90	75
4	C-4	97	97	364
5	C-5	30	30	26
6	C-6 ^[c]	39	39	18
7	C-7 ^[c]	39	39	19

[a] Reaction conditions: catalyst (0.01 mmol), formic acid (0.4 M, 2.5 mL), HCOONa (0.05 mmol), 90 °C. [b] Based on the total gas released. [c] Catalyst (0.005 mmol). [d] TOF/TON per Ru atom.

Further, dehydrogenation of formic acid (0.4 M, 2.5mL) was performed over the active complexes **C-2** and **C-4** (1 mol%), using a varying amount of sodium formate (0.05 to 3 equivalents) (Table S2, entries 1-14 and Figure 1). Results inferred that the TOF could be enhanced to 514 h⁻¹ for complex **C-4** using [HCOONa]/[HCOOH] ratio of 2:1 (Table S2, entry 12). Further, a maximum initial TOF of 940 h⁻¹ was achieved with **C-4** for formic acid (2.0 M, 2.5 mL) and [HCOONa]/[HCOOH] ratio of 2:1. Moreover, the complex **C-4** was recycled for five consecutive catalytic runs for formic acid dehydrogenation reaction, with a TON of 2248, at 90 °C [HCOONa]/[HCOOH] ratio of 2:1 (Figure 2). These results suggest that the catalyst **C-4** was quite stable and does not lose its catalytic activity even after using it continuously for 15 hours under the catalytic reaction condition.

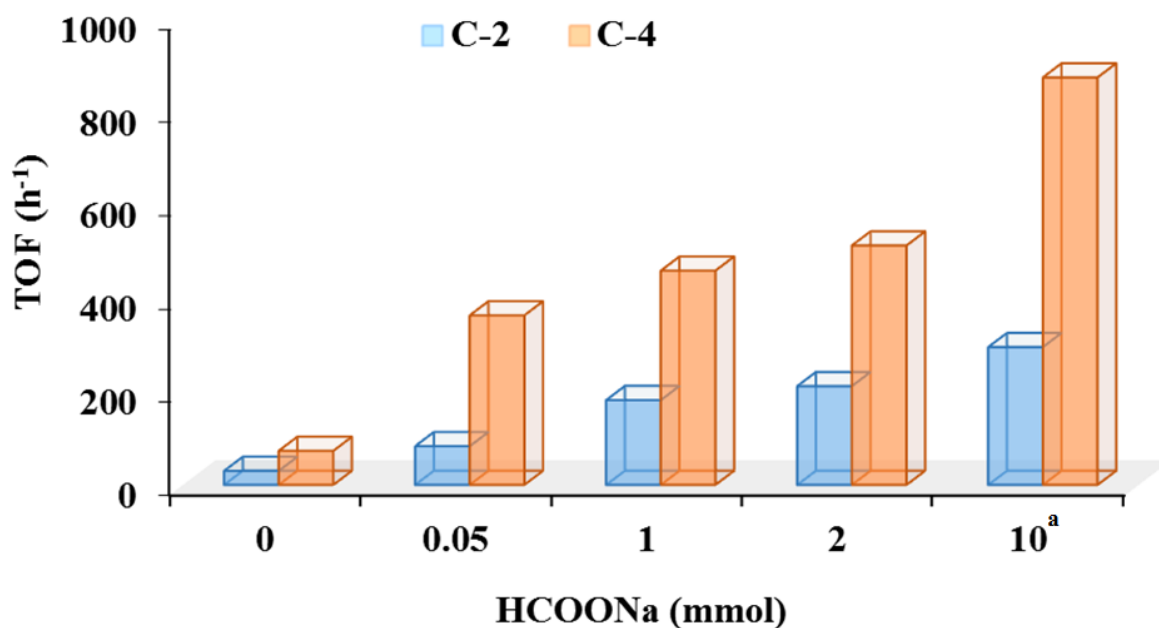


Figure 1. TOF (h⁻¹) vs [HCOONa] (mmol) plot for the catalytic dehydrogenation of formic acid over complexes **C-2** and **C-4**. Reaction conditions: formic acid (0.4 M, 2.5 mL), catalyst (0.01 mmol), 90 °C. [a] formic acid (2.0 M, 2.5 mL).

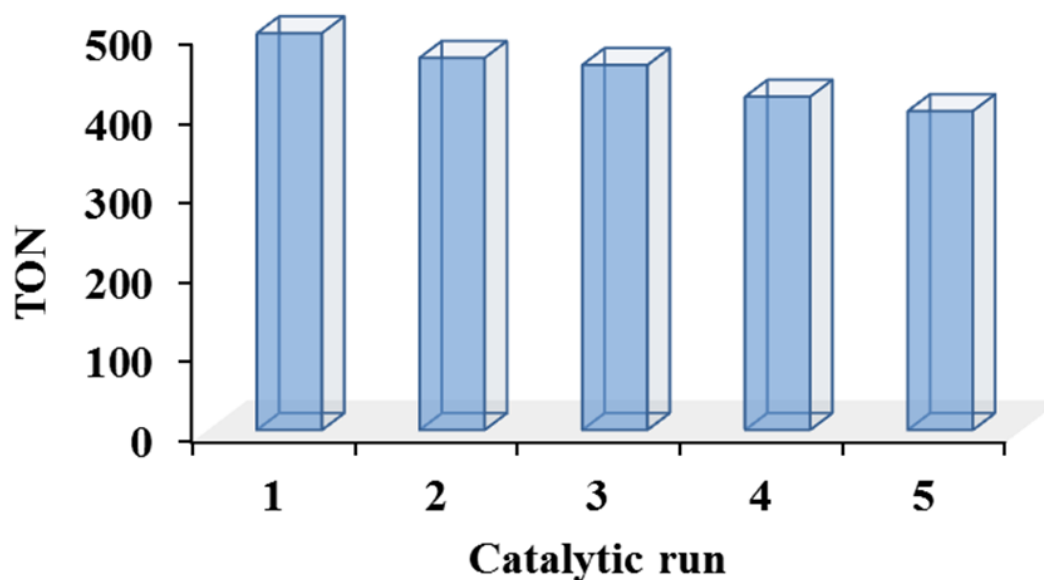


Figure 2. TON of the catalytic recyclability (1-5 catalytic runs) experiment for the catalytic dehydrogenation of formic acid over the complex **C-4**. Reaction conditions: formic acid (2.0 M, 2.5 mL), **C-4** (0.01 mmol), [HCOONa]/[HCOOH] = 2:1, 90 °C. (5 mmol of formic acid was added to the reaction mixture after each run).

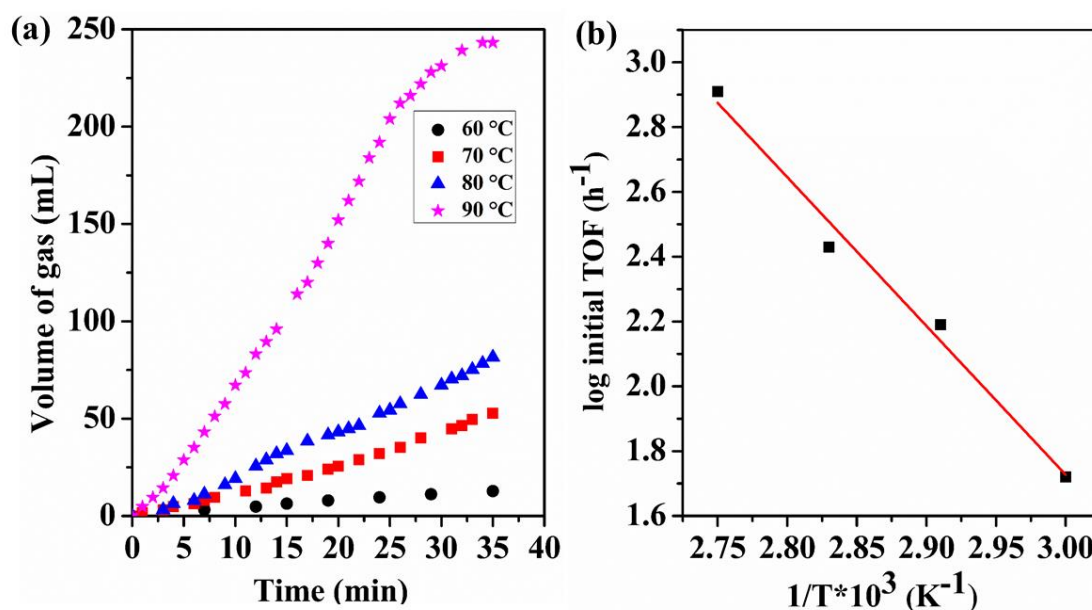


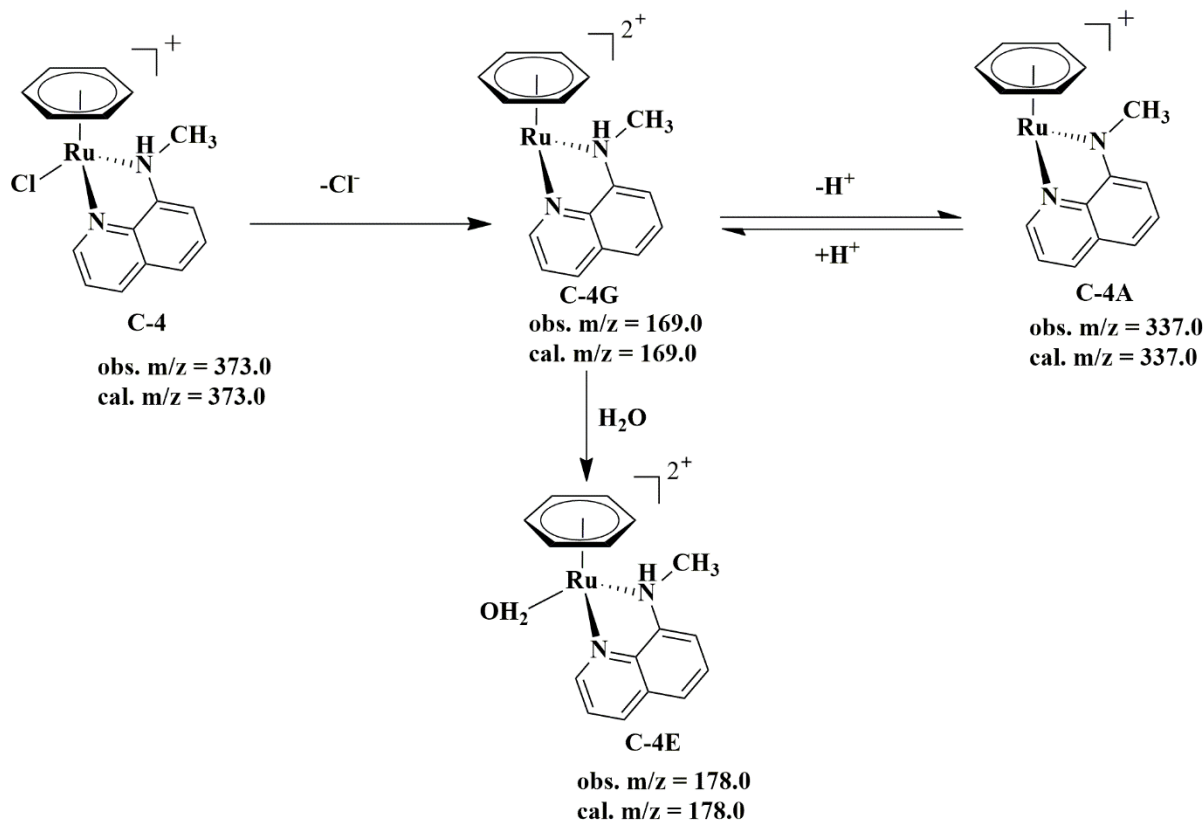
Figure 3. (a) Temperature dependent formic acid decomposition over **C-4** (1 mol %), formic acid (2M, 2.5 mL), HCOONa/ HCOOH = 2:1, T = 60 – 90 °C. (b) Arrhenius plot of initial TOF values for formic acid (2M, 2.5 mL) decomposition over **C-4** (1 mol%), HCOONa/ HCOOH = 2:1.

Further, the dependence of the rate of formic acid dehydrogenation on temperature, catalyst, and formic acid concentration was studied. The initial rates for the formic acid dehydrogenation over complex **C-4** followed Arrhenius behavior in the temperature range of 60 – 90 °C (Figure 3). The obtained apparent activation energy of 87.9 kJ/mol is in line with the activation energies reported for formic acid dehydrogenation over the analogous system.^[9] Subsequently, the dependence of the rate of formic acid dehydrogenation on the catalyst concentration was determined by varying the catalyst concentration between 0.005 mmol and 0.03 mmol, while keeping the formic acid concentration constant (2.0 M, 2.5 mL) at 90 °C. The double logarithmic plots of the initial reaction rates against the concentration of **C-4** catalyst follows a linear dependence on catalyst concentration. The obtained order of 0.8 with respect to catalyst concentration (Figure S3) suggests that **C-4** is converted into the

active monomeric species during the induction period and presumably the monomeric species is only involved in the formic acid dehydrogenation reaction. Further, the reaction order with respect to formic acid concentration, varied between 0.4 M and 2 M with a constant catalyst concentration of 0.01 mmol in 2.5 mL of aqueous solution at 90 °C, was found to be 0.31 (Figure S4). This result most probably indicates that only one formic acid or HCOO^- is interacting with the Ru center to form an $[\text{HCOO-Ru}]$ intermediate species.^[11,19] Also, no change in formic acid dehydrogenation efficiency over complex **C-4** was observed in the presence of excess metallic mercury, suggesting that the reaction follows a homogeneous pathway.

Based on the observations of the kinetic studies, attempts were made to systematically investigate and identify various organometallic intermediates presumably involved in the catalytic dehydrogenation of formic acid over Ru-catalyst using mass spectrometry. Stirring catalyst **C-4** in H_2O at room temperature showed few prominent mass peaks at $m/z = 169.0$ and 178.0 , which were assigned to **C-4G** and **C-4E**, respectively (Scheme 2 and Figure S5). The coordination of a H_2O molecule to the dicationic species, $[(\eta^6\text{-C}_6\text{H}_6)\text{Ru}(\kappa^2\text{-N}_{\text{py}}\text{NHMe-MAmQ})]^{2+}$ (**C-4G**; $m/z = 169.0$) gives a dicationic species $[(\eta^6\text{-C}_6\text{H}_6)\text{Ru}(\kappa^2\text{-N}_{\text{py}}\text{NHMe-MAmQ})(\text{H}_2\text{O})]^{2+}$ (**C-4E**; $m/z = 178.0$) in aqueous solution. Upon stirring an aqueous solution of **C-4** in the presence of sodium formate at room temperature, prominent mass peak at $m/z = 337.0$ was observed, which was assigned to $[(\eta^6\text{-C}_6\text{H}_6)\text{Ru}(\kappa^2\text{-N}_{\text{py}}\text{NMe-MAmQ})]^+$ (**C-4A**) species (Figure S6). The analogous, mass profile was also observed for **C-2** under identical reaction conditions (Figure S7). An H_2O coordinated dicationic $[(\eta^6\text{-C}_6\text{H}_6)\text{Ru}(\kappa^2\text{-N}_{\text{py}}\text{NH}_2\text{-AmQ})(\text{H}_2\text{O})]^{2+}$ (**C-2E**; $m/z = 171.0$) species was observed upon stirring the complex **C-2** in H_2O . Further, an intense peak corresponding to **C-2A** ($[(\eta^6\text{-C}_6\text{H}_6)\text{Ru}(\kappa^2\text{-N}_{\text{py}}\text{NH-AmQ})]^+$; $m/z = 323.0$), a species similar to **C-4A**, was also observed upon stirring the complex **C-2** in the

presence of sodium formate. Mass study of the dehydrogenation reaction with complex **C-2** in the presence of sodium formate also revealed **C-2A** ($[(\eta^6\text{-C}_6\text{H}_6)\text{Ru}(\kappa^2\text{-NpyNH-AmQ})]^+$) as the main metallic species formed in the reaction mixture (Figure S8). These observations, suggest that the presence of formate species facilitated the deprotonation of the N-H of the 8-aminoquinoline based ligands to form a coordinatively unsaturated **C-2A/C-4A** species.



Scheme 2. Various intermediate species observed during the mass investigation of an aqueous solution of complex **C-4** under varying controlled reaction condition.

The equilibria between the species **C-4G** and **C-4A** (for catalyst **C-4**) and **C-2G** and **C-2A** (for catalyst **C-2**) observed during the mass investigation (Scheme 2 and Figures S5 and S7) are pH sensitive and hence a pH-dependent study on the initial TOFs was conducted. The results showed that the highest TOF was achieved at pH = 4.0 (Figure 4), where the initial concentration of $[\text{HCOONa}]/[\text{HCOOH}]$ was fixed at 2:1 and hence the concentration

of such coordinatively unsaturated species **C-4A/C-2A** is expected to be high indicating that it may have a vital role in the catalytic cycle. The highest TOF obtained at moderately acidic condition indicates the importance of both H_3O^+ ions as well as HCO_2^- species in the dehydrogenation reaction.

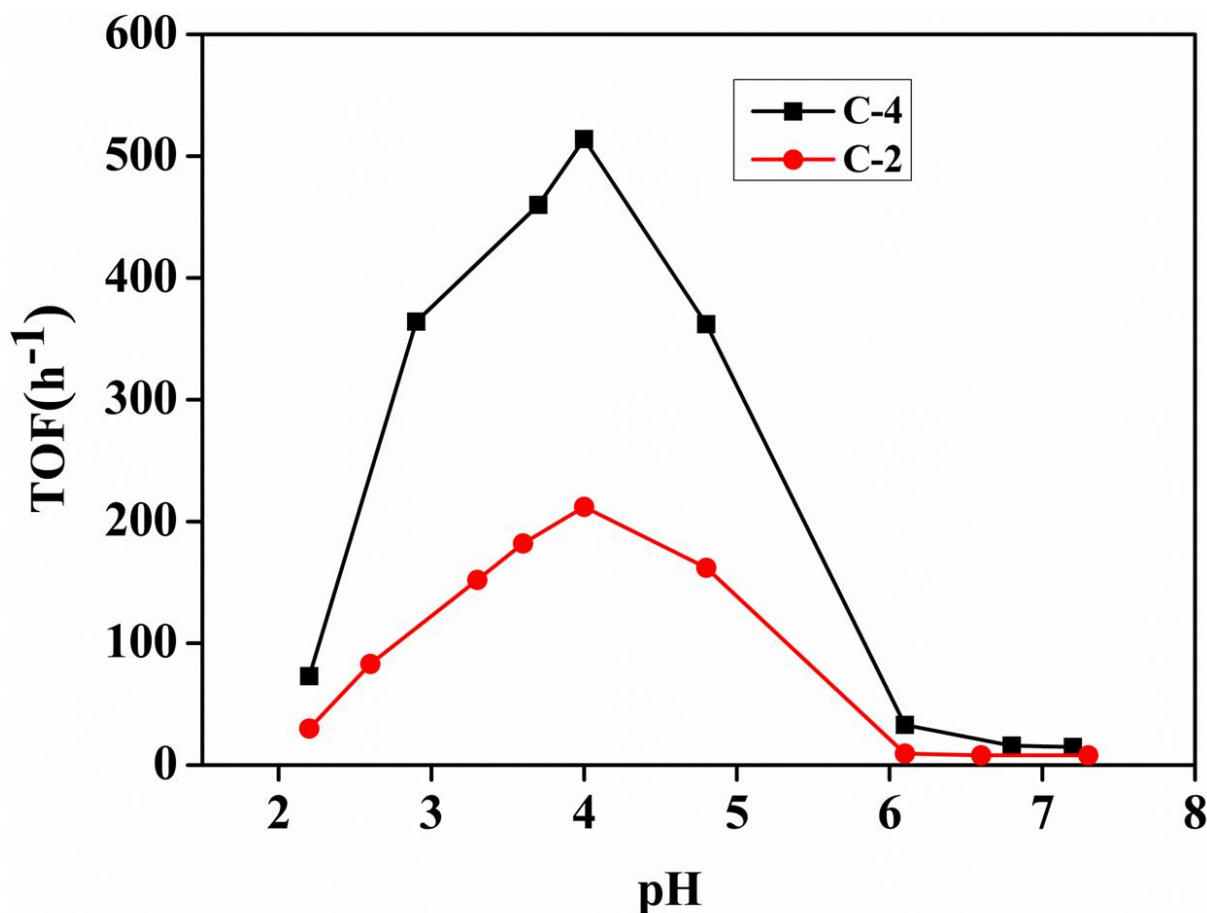
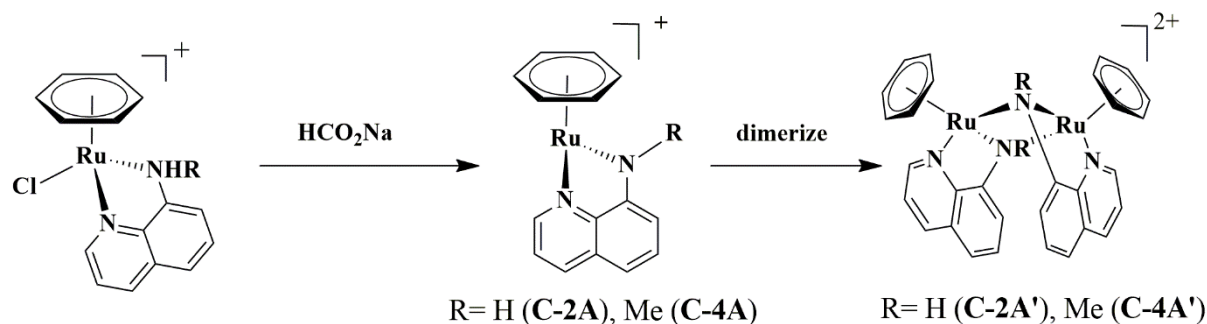


Figure 4. Dehydrogenation of formic acid under varying pH values, where pH values are altered by changing the $[\text{HCOONa}]/[\text{HCOOH}]$ ratios. Reaction condition: catalyst **C-2/C-4** (0.01 mmol), formic acid (0.4 M, 2.5 mL), $T = 90\text{ }^\circ\text{C}$.

To further confirm, the formation of the unsaturated species **C-2A** and **C-4A** in the presence of HCOONa , controlled reactions were performed. Treating complex **C-2** with an excess of sodium formate in methanol under reflux condition also led us to obtain **C-2A**. Further, orange colored block-shaped single crystals suitable for X-ray diffraction analysis

were obtained by slow diffusion of diethyl ether into the methanolic solution of **C-2A**. It is evident that the treatment of **C-2/C-4** with sodium formate led to the formation of the species **C-2A/C-4A**, which eventually dimerize to the stable diruthenium complex **C-2A'/C-4A'**, plausibly the catalyst resting state (Scheme 3).^[10g,20-22] Analogous unsaturated species $[\text{Ru}(\eta^6\text{-C}_{10}\text{H}_{14})(\text{Imd-H})]^+$ (Imd = 2,2'-bi-2-imidazole), generated *in situ* from $[\text{Ru}(\eta^6\text{-C}_{10}\text{H}_{14})\text{Cl}(2,2'\text{-bi-2-imidazole})]^+$ in the presence of sodium formate, was reported to play an important role in the formic acid dehydrogenation process.^[9] Interesting to note here, that literature also revealed that such coordinatively unsaturated species are unstable and may undergo dimerization.^[20-22] Similar dimeric species are also reported by Carmona *et al.*, where treatment of acetone solution of the complex $[(\eta^6\text{-C}_{10}\text{H}_{14})\text{Ru}(\kappa^2\text{-N}_{\text{py}}\text{OH})\text{Cl}]^+$ with Na_2CO_3 afforded dimer $[\{(\eta^6\text{-C}_{10}\text{H}_{14})\text{Ru}(\kappa^2\text{-N,O-}\mu\text{-O-NO})\}_2]^{2+}$.^[20] Valerga *et al.* also reported the crystal structure of a dinuclear Cp* ruthenium (III) complex $[\{\text{Cp}^*\text{Ru}(\kappa^2\text{-N,S-}\mu\text{-S-SC}_5\text{H}_4\text{N})\}_2]^{2+}$ while attempting to crystallize hydrido(alkoxo) derivative.^[21] Nishibayashi *et al.* reported similar species which are particularly relevant in the context of catalytic propargylation reaction of ketones.^[22]



Scheme 3. A plausible route to the diruthenium species (**C-2A'/C-4A'**), the catalyst resting state, via the coordinatively unsaturated species **C-2A/C-4A**.

The NMR spectra of **C-2A'** are consistent with the presence of deprotonated NH_2 ligand, and only one set of resonances was observed in the ^1H and ^{13}C NMR spectra

indicating the chemical equivalence of the two halves of the molecule (Figure S9). The single crystal X-ray structural determination showed that the asymmetric unit of **C-2A'** [$\{(\eta^6\text{-benzene})\text{Ru}(\kappa^2\text{-N}_{\text{py}}\text{NH-AmQ})\}_2\}^{2+}$] is formed by two units of $\{(\eta^6\text{-benzene})\text{Ru}(\kappa^2\text{-N}_{\text{py}}\text{NH-AmQ})\}^+$ (**C-2A**), where two $(\eta^6\text{-benzene})\text{Ru}$ units are doubly bridged by -NH groups of two 8-AmQ ligands (Figure 5 and Table S3-S5). The ruthenium bound $\eta^6\text{-benzene}$ ligands are placed at the mutually cisoid position. The center Ru-N-Ru-N core has a bent butterfly-like structure, with the dihedral angle of 151.44° between the two RuN_2 planes, presumably due to the steric crowding of the cisoid positioned $\eta^6\text{-benzene}$ rings. Moreover, the Ru1-N2-Ru2 bond angle is 97.28° , which is slightly larger than the reported values, indicating a weak interaction between two Ru centers having a Ru- Ru distance of 3.2 Å. The Ru-N_{amido} bond lengths of the two ruthenium units in the complex **C-2A'** are not same, suggesting the asymmetry in the coordination of N_{amido} with the two ruthenium centers. In particular, the Ru1-N4 (2.157 Å) and Ru2-N2 (2.158 Å) bonds (distances between the ruthenium center and the bridging N_{amido} from the other ruthenium unit) are significantly longer than the Ru1-N2 (2.106 Å) and Ru2-N4 (2.094 Å) bonds, further suggesting that two units of $\{(\eta^6\text{-benzene})\text{Ru}(\kappa^2\text{-N}_{\text{py}}\text{NH-AmQ})\}^+$ are weakly interacted via the two bridging N_{amido} groups. Notably, the Ru-N_{py} bond lengths in **C-2A'** are analogous to that observed in the monometallic complex **C-2**, while the Ru-N_{amido} bond lengths are quite short in comparison to Ru-N_{amine} bond in the monometallic complex **C-2**.^[19] Though the carbon atoms in the $\eta^6\text{-benzene}$ rings show some distortion due to the occupancy factors, the overall structure of the diruthenium complex **C-2A'** is well in accordance with literature reported analogous dimeric complexes.^[20-22]

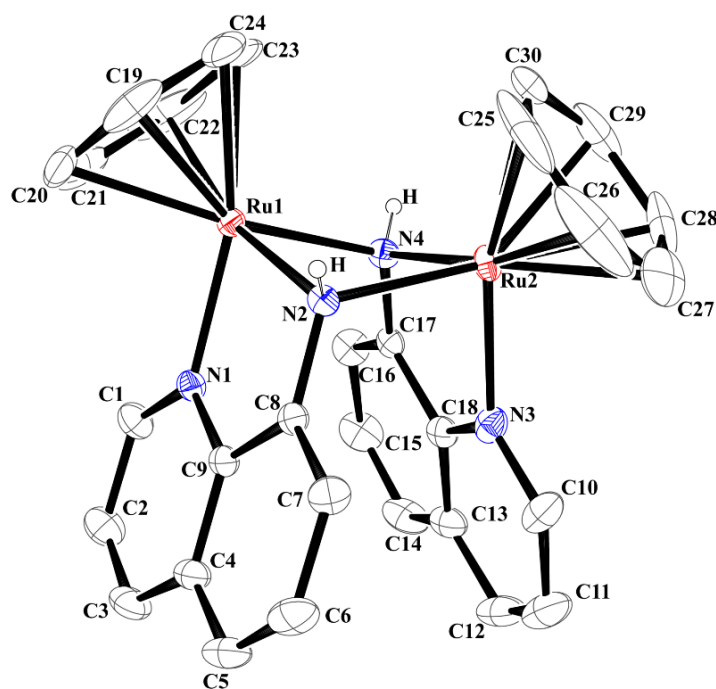


Figure 5. Single crystal X-ray structure of the diruthenium **C-2A'**. Counter anions (Cl^-) and all hydrogen atoms of **C-2A'**, except those on nitrogen, are omitted for clarity. Selected bond lengths (\AA) and angles ($^\circ$): Ru1-N4 2.157 (4), Ru2-N4 2.094(4), Ru1-N2 2.106(4), Ru2-N2 2.158(4), Ru1-N2-Ru2 97.28(16), Ru1-N4-Ru2 97.67(16), N2-Ru1-N4 77.94(15), N4-Ru2-N2 78.18(15).

Interesting to note that during the catalytic reaction, at first instance, a visible color change from a deep green solution of the catalysts **C-2/C-4** to a brown solution was observed during the initial minutes of the base-assisted catalytic dehydrogenation of formic acid (Figure S10). It should be noted that the observed brown color of the catalytic reaction was quite stable and we could not observe the initial green color of the solution even after the complete dehydrogenation of formic acid. Mass investigation of the brown solution showed the presence of **C-2A/C-4A** species. Further, the addition of an excess of dilute HCl in the obtained brown solution led to the regeneration of the initial green color. Mass spectral

analysis of the obtained green solutions depicted the presence of prominent peaks at m/z 359.0 and m/z 373.0, corresponding to **C-2** and **C-4**, respectively (Figure 6 and Figure S10).

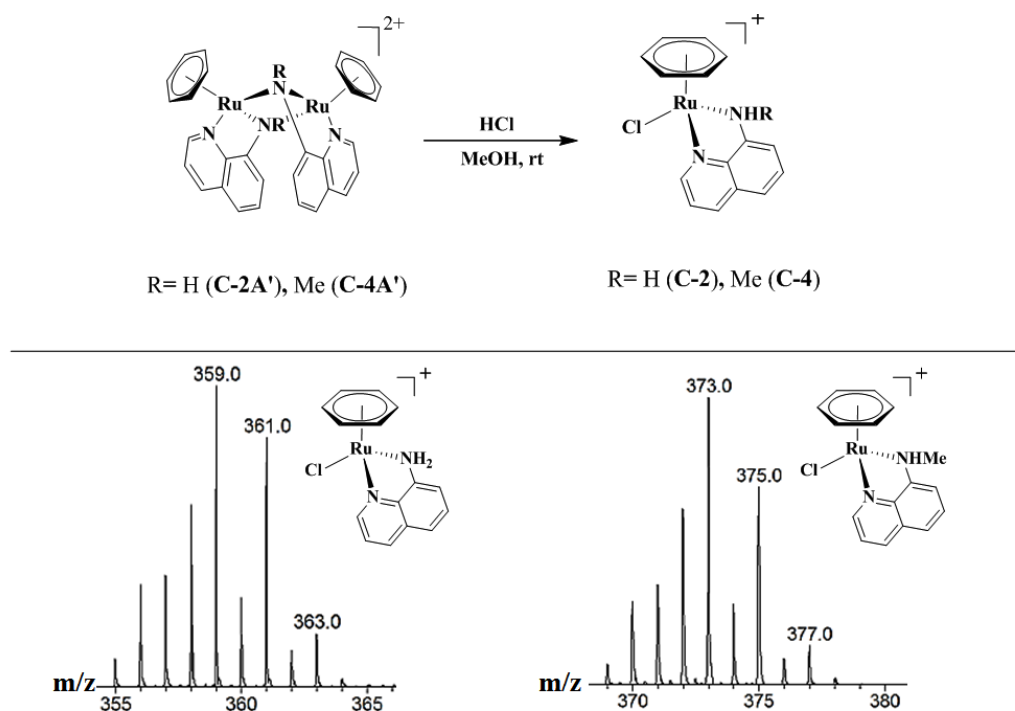


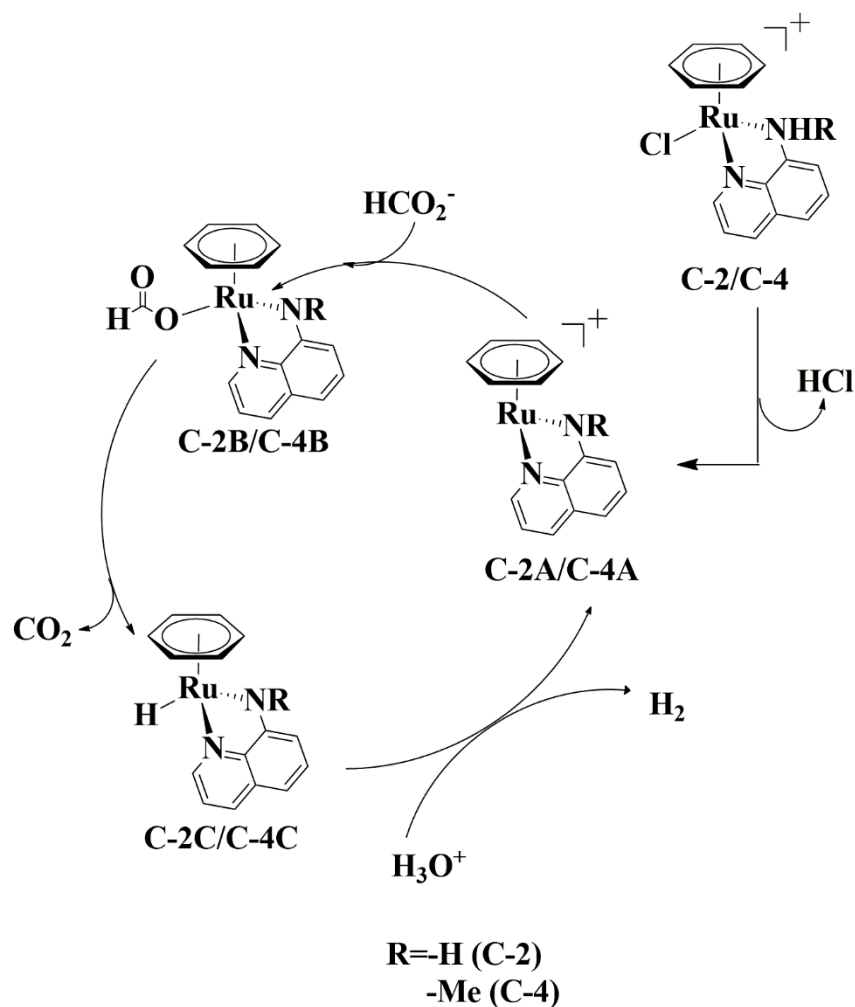
Figure 6. Mass investigation of the green-colored solutions obtained by the addition of an excess of dilute HCl to the brown solution after the catalytic reaction for **C-2** and **C-4**.

The above findings inferred that, upon treatment with HCOONa, **C-2/C-4** *in situ* transformed to the species **C-2A/C-4A**, which further reacted with formic acid/sodium formate to form formate coordinated Ru species (**C-2B/C-4B**).^[23] A Ru-hydride species **C-2C/C-4C** is expected to be formed, upon extrusion of CO₂ from **C-2B/C-4B**. This step is most probably the rate determining step in the catalytic cycle as indicated by kinetic isotope effect studies, where the deuterated formic acid (DCOOD) substrate (KIE: 2.9, Table 2, entry 3) is more influential than deuterated H₂O (D₂O) (KIE: 1.9, Table 2, entry 2) on the reaction rate, indicating that C-H bond cleavage of formic acid is the rate determining step.^[9,11]

Table 2. KIE in the dehydrogenation of formic acid using complex C-2 and C-4 ^[a]					
Entry	Catalyst	Substrate	Solvent	TOF (h ⁻¹) ^[b]	KIE ^[c]
1	C-4	HCOOH	H ₂ O	75	-
2	C-4	HCOOH	D ₂ O	40	1.9
3	C-4	DCOOD	H ₂ O	26	2.9
4	C-4	DCOOD	D ₂ O	22	3.4

^[a]Reaction conditions: Catalyst (0.01 mmol), formic acid (0.4 M, 2.5 mL), 90 °C;
^[b]TOF was calculated in the initial 1 hour; ^[c]KIE = TOF (entry 1)/ TOF (entry n)
(n = 2,3,4)

Further, upon the release of H₂ from the Ru-hydride species (**C-2C/C-4C**), the intermediate **C-2A/C-4A** was regenerated (Scheme 4). All our attempts to detect and isolate these Ru-formate or Ru-hydride species were unsuccessful. The indirect evidence for the formation of Ru-hydride species was gathered by utilizing the Ru-hydride species (**C-2C**) in the transfer hydrogenation of *p*-anisaldehyde to obtain corresponding alcohol under identical reaction condition (Figure S11).^[24] On the other hand, during base-free catalytic dehydrogenation of formic acid, a H₂O coordinated dicationic ruthenium species (**C-2E/C-4E**) was possibly generated, as also evidenced by the appearance of a mass peak at *m/z* = 171.0 (**C-2E**) and *m/z* = 178.0 (**C-4E**) (Figures S5 and S7). Further, formate replaces H₂O from **C-2E/C-4E** resulting in the formation of the species **C-2F/C-4F**. Hydride species **C-2D/C-4D** is formed after the decarboxylation of Ru-formate species (**C-2F/C-4F**). The H₂O coordinated dicationic ruthenium species (**C-2E/C-4E**) will be regenerated, upon the proton-assisted release of H₂ from **C-2D/C-4D**. Based on the above mass studies and x-ray crystal structure, we propose a plausible pathway for both the base-free and base-assisted dehydrogenation of formic acid over complexes **C-2** and **C-4** (Scheme S3).^[4k,9]



Scheme 4. A plausible catalytic pathway for the base assisted formic acid dehydrogenation over complexes **C-2** and **C-4**.

Conclusions

In summary, we employed several Ru-arene complexes for the catalytic dehydrogenation of formic acid in H_2O , where the complex **C-4** containing 8-(N-methylamino)quinoline ligand outperformed over others to achieve a TON of 2248. The high activity of **C-4** can be attributed to the high aqueous stability of the catalyst and availability of -NH moiety. Further, we employed extensive mass and NMR investigations and kinetic studies to evidence the formation of several important organometallic intermediate species, such as H_2O coordinated dicationic ruthenium species $[(\eta^6\text{-C}_6\text{H}_6)\text{Ru}(\kappa^2\text{-NpyNHMe-MAmQ})(\text{H}_2\text{O})]^{2+}$ (**C-4E**) and the

active coordinatively unsaturated species $[(\eta^6\text{-C}_6\text{H}_6)\text{Ru}(\kappa^2\text{-N}_{\text{py}}\text{NMe-MAmQ})]^+$ (**C-4A**) during the catalytic dehydrogenation of formic acid over complex **C-4**, and hence, established their important role in the catalytic dehydrogenation of formic acid. Most importantly, we succeeded in isolating the plausible catalyst resting state and characterized it as a dicationic diruthenium species (**C-2A'**), by single crystal X-ray diffraction.

Experimental Section

Materials and instrumentation. All reactions were performed in aerobic conditions using high-purity chemicals purchased from Sigma-Aldrich, and Alfa-Aesar. ^1H NMR (400 MHz), ^{13}C NMR (100 MHz) spectra were recorded at 298 K using D_2O and CDCl_3 as solvents on a Bruker advance 400 spectrometer. ESI-mass spectra were recorded on a micrOTF-Q II mass spectrometer. The GC-TCD analysis was performed on a Shimadzu GC-2014 system using shin carbon-ST packed column.

Synthesis of the ligand 8-(N-methylamino)quinoline. To the freshly prepared solution of NaOMe (20 mmol) in MeOH (20 mL), 8-aminoquinoline (4 mmol) and paraformaldehyde (20 mmol) were added. The mixture was allowed to reflux for 4 hours, and NaBH_4 (6 mmol) was added portion wise at 0°C and the mixture was refluxed for an additional 2 hours. The completion of the reaction analyzed by TLC, the mixture was cooled, and the solvent was evaporated on a vacuum pump to give a residue that was treated with an aqueous layer (20 mL). The compound was extracted with dichloromethane (2×15 mL). The organic residue was dried over anhydrous Na_2SO_4 , and the solvent was removed using vacuum pump and residue that was purified through silica gel column chromatography with hexane/ethyl acetate (9.5: 0.5 v/v) to obtain the pure product. Yellow color. ^1H NMR (400 MHz, CDCl_3): δ (ppm) = 8.70 (d, 1H, $J=4$ Hz), 8.06 (d, 1H, $J=8$ Hz), 7.42- 7.35 (m, 2H), 7.05 (d, 1H, $J=8$ Hz), 6.65 (d, 1H, $J=8$ Hz), 6.12 (br, 1H), 3.04 (d, 3H, $J=4$ Hz).

Synthesis of the complex C-4. The ligand 8-(N-methylamino)quinoline (1.1 mmol) was dissolved in 30 mL MeOH taken in a 100 mL round-bottomed flask and $[(\eta^6\text{-benzene})\text{RuCl}_2]_2$ (0.5 mmol) was added to it. The mixture was stirred for 24 h at room temperature after which the volume of solvent was reduced on a vacuum pump. The complex was precipitated out with diethyl ether, washed several times to get rid of the excess ligand. It was then dried and collected. Colour: Deep green. Yield 68%. ^1H NMR (400 MHz, D_2O): δ (ppm) = 9.38 (dd, $J = 30.3, 5.1$ Hz, 1H), 8.25 (t, $J = 7.1$ Hz, 1H), 7.63 (d, $J = 7.6$ Hz, 2H), 7.43 (dd, $J = 10.4, 8.3$ Hz, 2H), 5.96 – 5.75 (m, 6H), 3.06 (s, 3H). ^{13}C NMR (100 MHz, D_2O): δ (ppm) = 129.34, 128.25, 127.75, 127.36, 126.51, 125.57, 124.27, 123.97, 123.71, 85.48, 85.35, 48.81. MS (ESI) m/z calculated for $[(\eta^6\text{-C}_6\text{H}_6)\text{Ru}(\kappa^2\text{-N}_{\text{py}}\text{NHMe-MAmQ})\text{Cl}]^+$: 373.0 $[\text{M}]^+$, found 373.0 $[\text{M}]^+$

Controlled experiment for the synthesis of C-2A'. Complex **C-2** (0.2 mmol) and HCOONa (0.4 mmol) in methanol (25 mL) were refluxed for 1 h till a visible color change from green to brown was observed. The resulting solution was filtered, and the solvent was removed under reduced pressure to obtain **C-2A'**. Colour: Brown. Yield 73%. ^1H NMR (400 MHz, D_2O): δ (ppm) = 8.12 (d, 1H, $J = 8$ Hz), 7.82 (d, 2H, $J = 8$ Hz), 7.51 (t, 1H, $J = 6$ Hz), 7.16 (d, 1H, $J = 8$ Hz), 6.87-6.84 (m, 1H), 5.74 (s, 6H). ^{13}C NMR (100 MHz, D_2O): δ (ppm) = 155.32, 153.91, 144.06, 137.44, 128.06, 127.99, 122.96, 122.20, 120.75, 85.27.

Single-Crystal X-ray Diffraction Studies. A Single crystal was obtained by diffusion of diethyl ether into a methanol solution of **C-2A'**. X-ray structural studies of **C-2A'** were executed on a CCD Agilent Technologies (Oxford Diffraction) SUPERNOVA diffractometer. Using graphite-monochromated $\text{Cu K}\alpha$ radiation ($\lambda = 1.54184 \text{ \AA}$)-based diffraction, data were collected at 293(2) K by the standard “phi-omega” scan techniques and were scaled and reduced using CrysAlisPro RED software. The extracted data were evaluated

using the CrysAlisPro CCD software. The structures were solved by direct methods using SHELXL-2018/1, and refined by full-matrix least squares method, refining on F^2 .^[25] The positions of all of the atoms were determined by direct methods. All non-hydrogen atoms were refined anisotropically. The remaining hydrogen atoms were placed in geometrically constrained positions. The CCDC number 1810973 contains the supplementary crystallographic data for **C-2A'**. These data are freely available at www.ccdc.cam.ac.uk (or can be procured from the Cambridge Crystallographic Data Centre, 12 Union Road, Cambridge CB21 EZ, UK; fax: (+44) 1223-336-033; or deposit@ccdc.cam.ac.uk).

The General process for formic acid dehydrogenation reactions. To an aqueous solution (2.5 mL) of complex **C-4/C-2** (0.01 mmol) was added HCOONa (0.05 mmol) in a two-necked reaction tube fitted with a condenser and a gas burette. Further, HCOOH (1 mmol) was added to the reaction mixture and was heated at 90 °C. The release of gas was measured as the displacement of H₂O in the burette. The release of H₂ gas was confirmed by GC-TCD.

The process for recycling experiments. Formic acid (2.0 M, 2.5 mL), **C-4** (0.01 mmol), [HCOONa]/[HCOOH] = 2:1 was taken in a two-necked test tube and heated at 90 °C. The gas released was calculated by the water displacement method. After the release of gas stopped, 5 mmol of formic acid was added to the reaction mixture after each run, and the release of gas monitored.

The General process for the mechanistic studies. NMR and mass spectral studies were performed for the identification of various catalytic species involved in the catalytic dehydrogenation of formic acid over the complex **C-2** and **C-4**. The species **C-2A/C-4A** and **C-2E/C-4E** was identified by mass spectrometry from an aqueous solution of **C-2/C-4** under varying reaction conditions.

Acknowledgments

Authors gratefully acknowledge the financial support from IIT Indore, CSIR and SERB-DST. SIC, IIT Indore and Discipline of Chemistry are acknowledged for providing instrumentation facility. S.P., R.K.R, and S.K.S designed the project, S.P. conducted the experiments, H.D. and S.M.M. helped in X-ray refinement, S.P., M.K.A. and S.K.S. wrote the article. S.P. and M.K.A. thank MHRD and INSPIRE-DST, respectively for their fellowships. R.K.R thanks CSIR and IIT Indore for his fellowship. H.D. thanks SERB-DST for his N-PDF fellowship.

Conflict of interest

The authors declare no conflict of interest.

References

- [1] H. Zhang, P. K. Shen, *Chem. Rev.* **2012**, *112*, 2780–2832.
- [2] M. Pourbaba, S. Zirakkar, *Procedia Eng.* **2011**, *21*, 1088–1095.
- [3] a) A. F. Dalebrook, W. Gan, M. Grasmann, S. Moret, G. Laurenczy, *Chem. Commun.* **2013**, 8735-8751. b) M. Yadav, Q. Xu, *Energy Environ. Sci.* **2012**, *5*, 9698-9725. c) H. L. Jiang, S. K. Singh, J. M. Yan, X. B. Zhang, Q. Xu, *ChemSusChem.* **2010**, *3*, 541-549.
- [4] a) D. Mellmann, P. Sponholz, H. Junge, M. Beller, *Chem. Soc. Rev.* **2016**, *45*, 3954–3988. b) M. Grasmann, G. Laurenczy, *Energy Environ. Sci.* **2012**, *5*, 8171–8181. c) S. Enthaler, J. von Langermann, T. Schmidt, *Energy Environ. Sci.* **2010**, *3*, 1207–1217. d) T. C. Johnson, D. J. Morris, M. Wills, *Chem. Soc. Rev.* **2010**, *39*, 81–88. e) F. Joó, *ChemSusChem.* **2008**, *1*, 805–808. f) J. Eppinger, K. W. Huang *ACS Energy Lett.* **2017**, *2*, 188–195. g) A. K. Singh, S. Singh, A. Kumar, *Catal. Sci. Technol.* **2016**, *6*, 12-40. h) N. Onishi, G. Laurenczy, M. Beller, Y. Himeda, *Coordination Chemistry Reviews.* **2018**, *373*, 317-332. i) N. Onishi, M. Iguchi, X. Yang, R. Kanega, H.

- Kawanami, Q. Xu, Y. Himeda, *Adv. Energy Mater.* **2018**, 1801275. j) K. Sordakis, C. Tang, L. K. Vogt, H. Junge, P. J. Dyson, M. Beller, G. Laurenczy, *Chem. Rev.* **2018**, *118*, 372–433. k) M. Iglesias, L. A. Oro, *Eur. J. Inorg. Chem.* **2018**, 2125–2138.
- [5] R. Coffey, *Chem. Commun.* **1967**, 923–924.
- [6] a) I. Mellone, N. Gorgas, F. Bertini, M. Peruzzini, K. Kirchner, L. Gonsalvi, *Organometallics* **2016**, *35*, 3344–3349. b) E. A. Bielinski, P. O. Lagaditis, Y. Zhang, B. Q. Mercado, C. Würtele, W. H. Bernskoetter, N. Hazari, S. Schneider, *J. Am. Chem. Soc.* **2014**, *136*, 10234–10237. c) T. Zell, B. Butschke, Y. Ben-David, D. Milstein, *Chem. - Eur. J.* **2013**, *19*, 8068–8072.
- [7] a) S. Fukuzumi, T. Kobayashi, T. Suenobu, *ChemSusChem* **2008**, *1*, 827–834. b) Y. Himeda, S. Miyazawa, T. Hirose, *ChemSusChem* **2011**, *4*, 487–493. c) D. Jantke, L. Pardatscher, M. Dress, M. Cokoja, W. A. Herrmann, F. E. Kuhn, *ChemSusChem* **2016**, *9*, 2849–2854. d) Z. Wang, S. M. Lu, J. Wu, C. Li, J. Xiao, *Eur. J. Inorg. Chem* **2016**, *2016*, 490–496.
- [8] a) Y. Pan, C. L. Pan, Y. Zhang, H. Li, S. Min, X. Guo, B. Zheng, H. Chen, A. Anders, Z. Lai, J. Zheng, K.-W. Huang, *Chem. - Asian J.* **2016**, *11*, 1357–1360. b) M. Czaun, A. Goeppert, J. Kothandaraman, R. B. May, R. Haiges, G. K. S. Prakash, G. A. Olah, *ACS Catal.* **2014**, *4*, 311–320. c) A. Guerriero, H. Bricout, K. Sordakis, M. Peruzzini, E. Monflier, F. Hapiot, G. Laurenczy, L. Gonsalvi, *ACS Catal.* **2014**, *4*, 3002–3012. d) S. Fukuzumi, T. Kobayashi, T. Suenobu, *J. Am. Chem. Soc.* **2010**, *132*, 1496–1497. e) A. Boddien, B. Loges, H. Junge, F. Gärtner, J. R. Noyes, M. Beller, *Adv. Synth. Catal.* **2009**, *351*, 2517–2520. f) C. Fellay, P. J. Dyson, G. Laurenczy, *Angew. Chem., Int. Ed.* **2008**, *47*, 3966–3968. g) B. Loges, A. Boddien, H. Junge, M. Beller, *Angew. Chem., Int. Ed.* **2008**, *47*, 3962–3965. h) C. Fellay, N. Yan, P. J. Dyson, G. Laurenczy, *Chem. - Eur. J.* **2009**, *15*, 3752–3760. i) A. Boddien, C. Federsel, P. Sponholz, D. Mellmann, R.

- Jackstell, H. Junge, G. Laurenczy, M. Beller, *Energy Environ Sci.* **2012**, *5*, 8907-8911.
- j) P. Sponholz, D. Mellmann, H. Junge, M. Beller, *ChemSusChem.* **2013**, *6*, 1172-1176.
- [9] C. Guan, D. Zhang, Y. Pan, M. Iguchi, M.J. Ajitha, J. Hu, H. Li, C. Yao, M. H. Huang, S. Min, J. Zheng, Y. Himeda, H. Kawanami, K. W. Huang, *Inorg Chem.* **2017**, *56*, 438-445.
- [10] a) J. J. A. Celaje, Z. Lu, E. A. Kedzie, N. J. Terrile, J. N. Lo, T. J. A. Williams, *Nat. Commun.* **2016**, *7*, 11308–11313. b) M. Czaun, J. Kothandaraman, A. Goepfert, B. Yang, S. Greenberg, R. B. May, G. A. Olah, G. K. S. Prakash, *ACS Catal.* **2016**, *6*, 7475–7484. c) A. Matsunami, Y. Kayaki, T. Ikariya, *Chem. Eur. J.* **2015**, *21*, 13513–13517. d) S. Oldenhof, M. Lutz, B. de Bruin, J. I. van der Vlugt, J. N. H. Reek, *Chem. Sci.* **2015**, *6*, 1027-1034. e) Y. Manaka, W.-H. Wang, Y. Suna, H. Kambayashi, J. T. Muckerman, E. Fujita, Y. Himeda, *Catal. Sci. Technol.* **2014**, *4*, 34-37. f) E. Fujita, J. T. Muckerman, Y. Himeda, *Biochim. Biophys. Acta, Bioenerg.* **2013**, *1827*, 1031-1038. g) J. H. Barnard, C. Wang, N. G. Berry, J. L. Xiao, *Chem. Sci.* **2013**, *4*, 1234–1244. h) S. Oldenhof, B. de Bruin, M. Lutz, M. A. Siegler, F. W. Patureau, J. I. van der Vlugt, J. N. H. Reek, *Chem. - Eur. J.* **2013**, *19*, 11507-11511. i) R. Tanaka, M. Yamashita, L. W. Chung, K. Morokuma, K. Nozaki, *Organometallics* **2011**, *30*, 6742-6750. j) C. Fink, G. Laurenczy, *Dalton trans.* **2017**, *46*, 1670- 1676. k) M. Iguchi, H. Zhong, Y. Himeda, H. Kawanami, *Chem. - Eur. J.* **2017**, *23*, 1-6. l) S. M. Lu, Z. Wang, J. Wang, J. Li, C. Li, *Green Chem.* **2018**, *20*, 1835-1840. m) A. Matsunami, S. Kuwata, Y. Kayaki, *ACS Catal.* **2017**, *7*, 4479–4484. n) W.-H. Wang, S. Xu, Y. Manaka, Y. Suna, H. Kambayashi, J. T. Muckerman, E. Fujita, Y. Himeda, *ChemSusChem.* **2014**, *7*, 1976–1983. o) J. Li, J. Li, D. Zhang, C. Liu, *ACS Catal.* **2016**, *6*, 4746-4754. p) J. F. Hull, Y. Himeda, W. H. Wang, B. Hashiguchi, R. Periana, D. J. Szalda, J. T. Muckerman, E. Fujita, *Nat. Chem.* **2012**, *4*, 383-388. q) W. H. Wang, M. Z. Ertem, S.

- Xu, N. Onishi, Y. Manaka, Y. Suna, H. Kambayashi, J. T. Muckerman, E. Fujita, Y. Himeda, *ACS Catal.* **2015**, *5*, 5496-5504. r) M. Iguchi, Y. Himeda, Y. Manaka, H. Kawanami, *ChemSusChem.* **2016**, *9*, 2749-2753. s) R. Kanega, N. Onishi, L. Wang, K. Murata, J. Muckerman, E. Fujita, Y. Himeda, *Chem. - Eur. J.* **2018**, *24*, 1-5. t) G. Papp, G. Olveti, H. Horvath, A. Katho, F. Joo, *Dalton trans.* **2016**, *45*, 14516-14519.
- [11] Z. Wang, S. Lu, J. M. Li, J. Wang, C. Li, *Chem. - Eur. J.* **2015**, *21*, 12592–12595.
- [12] J. F. Hull, Y. Himeda, W.-H. Wang, B. Hashiguchi, R. Periana, D. J. Szalda, T. James, J. T. Muckerman, E. Fujita, *Nat. Chem.* **2012**, *4*, 383-388.
- [13] Y. Himeda, *Green Chem.* **2009**, *11*, 2018-2022.
- [14] A. Iturmendi, L. R- Perez, J J. Perez- Torrente, M. Iglesias, L. A. Oro, *Organometallics.* **2018**, DOI: 10.1021/acs.organomet.8b00289.
- [15] G. A. Filonenko, R. van Putten, E. N. Schulpen, E. J. Hensen, E. A. Pidko, *ChemCatChem.* **2014**, *6*, 1526–1530.
- [16] R. E. Rodriguez- Lugo, M. Trincado, M. Vogt, F. Tewes, G. Santiso- Quinones, H. Gritzmacher, *Nat. Chem.* **2013**, *5*, 342- 347.
- [17] K. Gupta, D. Tyagi, A. D. Dwivedi, S. M. Mobin, S. K. Singh, *Green Chem.* **2015**, *17*, 4618-4627.
- [18] A. D. Dwivedi, K. Gupta, D. Tyagi, R. K. Rai, S. K. Singh, *ChemCatChem.* **2015**, *7*, 4050- 4058.
- [19] A. Boddien, D. Mellmann, F. Gärtner, R. Jackstell, H. Junge, P. J. Dyson, G. Laurenczy, R. Ludwig, M. Beller, *Science* **2011**, *333*, 1733-1736.
- [20] D. Carmona, P. Lamata, A. Sanchez, P. Pardo, R. Rodriguez, P. Ramirez, F. J. Lahoz, P. Garcia-orduna, L. A. Oro, *Organometallics* **2014**, *33*, 4016-4026.
- [21] M. J. Tenorio, M. C. Puerta, P. Valerga, *Inorg. Chem.* **2011**, *50*, 12399-12401.

- [22] Y. Nishibayashi, H. Imajima, G. Onodera, Y. Inada, M. Hidai, S. Uemura, *Organometallics* **2004**, *23*, 5100– 5103.
- [23] I. Mellone, M. Peruzzini, L. Rosi, D. Mellmann, H. Junge, M. Beller, L. Gonsalvi, *Dalton trans.* **2013**, *42*, 2495-2501.
- [24] Z. Yang, Z. Zhu, R. Luo, X. Qiu, J. T. Liu, J. K. Yang, W. Tang, *Green Chem.* **2017**, *19*, 3296- 3301.
- [25] G. M. Sheldrick, *Acta crystallogr., Sect. A: Found. Crystallogr.* **2008**, *64*, 112-122.

(Table of Content)

Efficient catalytic dehydrogenation of formic acid was achieved over water-soluble Ru-arene complexes containing 8-aminoquinoline based ligands, where the role of NH moiety and the stability of catalytic species in H₂O plays important role in achieving high catalytic activity over $[(\eta^6\text{-C}_6\text{H}_6)\text{Ru}(\kappa^2\text{-N}_{\text{py}}\text{NHMe-MAmQ})\text{Cl}]^+$ (**C-4**). Moreover, extensive mass studies infer the involvement of a coordinatively unsaturated species **C-2A/C-4A** as the active component, which was isolated and characterized (by X-ray crystallography) as a diruthenium complexes.

